

Fatigue crack propagation in two dimensional lattice spring models

T.M. Guozden and E.A. Jagla

February 9, 2009

Centro Atómico Bariloche, Comisión Nacional de Energía Atómica (8400)
Bariloche, Argentina

Abstract

Fatigue crack propagation is studied in 2D lattice spring models in a stripe geometry under constant displacement boundary conditions, for multiple lattice geometries. The work is done in the presence of plasticity and in the absence of dynamic effects. Plasticity is modeled by changing the offset of the springs, in such a way as to keep the maximum force below a certain value. The springs fail if the total deformation surpasses some prescribed threshold. The results are compatible with the Paris law. The effects of overloading and small cracks are reproduced. A universal behavior for each kind of lattice is obtained by studying the relation between the breaking and plasticity thresholds.

1 Introduction

The aim of this work is to numerically study the process of fatigue crack advance [1] in the presence of cyclic loads and plasticity effects. The essence of cyclic plasticity can be described as follows: when an increasing load is applied to a crack the material first deforms elastically, until plastic deformation eventually occurs at the crack tip. As the load increases further, the crack starts to elongate. However, due to the effect of the plastic region, this elongation does not produce the immediate rupture of the sample, instead the crack elongation is a function of the applied load. Upon unloading the plastic deformation mostly reverts, leaving the crack ready to start a new elongation cycle in the next loading.

It is important to emphasize that the process being studied is fully deterministic, and that the crack advance is a consequence of cycling. Other approaches to fatigue crack advance, such as that in Ref. [2], focus on stochastic

effects in the material properties, but this is not of immediate interest for us in this work.

The material is modelled by a collection of point masses joined by springs. The springs will be given a deterministic plastic behavior that will be responsible for the cycle fatigue propagation. Dynamic effects (such as dependences on the time the load is applied) will not be considered. With these minimal inputs propagation according to a Paris law is obtained, and the overloading and small crack effects are observed[1].

2 Methods

Cracks in two dimensional spring-lattice samples are simulated using a mode III configuration. The model consists of an arrange of point particles linked by springs in a semi infinite stripe. The force exerted by a spring is $F = k(x - x_0)$, where x is distance between the masses attached to it, and x_0 is the spring rest length. Plasticity is modeled by changing x_0 in order to keep the force below some threshold $|F| < ku_{nl}$. An example of the evolution of F as x is changed in a prescribed manner is shown in Fig. [1]. Note that the evolution is deterministic, but the force is not an univocous function of x .

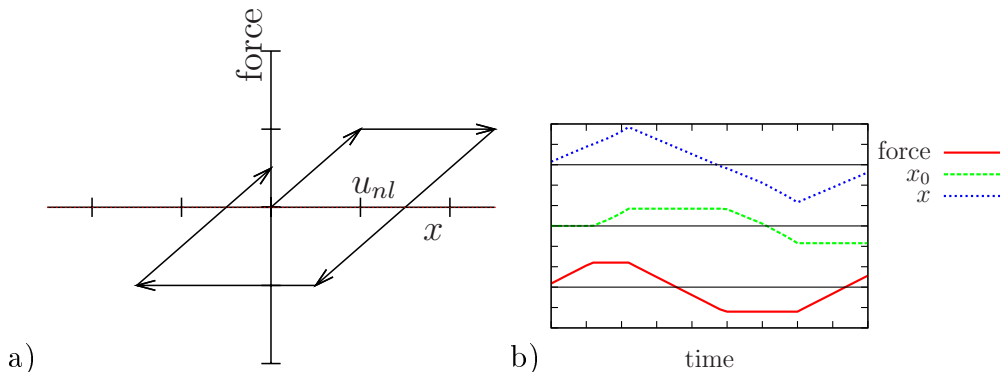


Figure 1: Plastic behavior of the springs. In *a*) the force of a spring when x increases and then decreases is shown schematically, and in *b*) the time evolution of force, length (x) and rest length (x_0) is indicated. Note that when the force reaches its maximum, x_0 starts to change.

Springs located in the middle of the stripe will fail if they are stretched above some quantity u_{bk} , i.e., if $|x| > u_{bk}$. This will force the propagation of the crack along the central line of the stripe. This models, for instance, propagation along a weak interface between two materials.

Results for different lattices are compared in Fig. [2]: square (in this case plasticity is introduced only on horizontal springs), rhomboidal (which is a square lattice rotated 45° , plasticity in all springs) and triangular (plasticity in all springs). Results for a square lattice in which plasticity is introduced not in spring variables but in element variables are also shown. The advantage

of this last implementation is that plasticity is essentially isotropic, and the results are expected to compare better with experimental data in continuous materials.

The dynamics is typically solved in the following way: fixing the conditions at the borders the model is evolved until equilibrium is reached. In this situation the boundary condition is changed a small step and the process is repeated. Some slight variations of this procedure are used in particular cases to speed up simulations. These variations are made only for computational advantage, and do not have any physical consequence.

2.1 Results

First of all the structure of the plastic region in a loaded crack at rest is analyzed, for each of the described lattices. For rhomboidal and square lattices (Figs. [2a] and [2b]) the plastic region consists of only two strings of springs. In contrast, triangular lattice (Fig. [2c]) shows a continuum region where springs enter the nonlinear region, as in the case of the square lattice with plasticity per elements (Fig. [2d]).

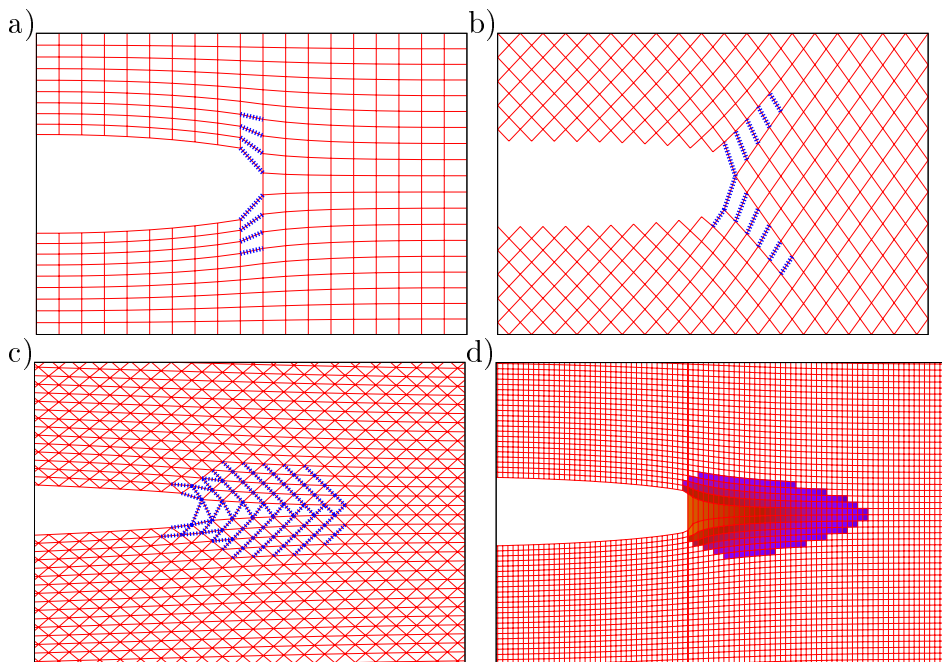


Figure 2: Plasticity in different lattices with a semi infinite crack under load (without propagation). *a*) square, *b*) rhomboidal, *c*) triangular, and *d*) square with plasticity per elements. Highlighted springs (or elements in *d*) are those in which plastic deformation is not zero. In *a*) and *b*) only one column of springs enters the plastic region while in *c*) and *d*) there is a continuum plastic region.

When cracks are allowed to elongate, the properties of different lattices are found to be different. Calculations are referred to the nominal values of the

stress intensity factor K attained at the crack tip, as obtained from L.E.F.M. There are some important reference values for K : K_{nl} is the stress intensity factor at which the first spring enters the plastic regime, K_{min} is the minimum value that is necessary to apply over a sample to observe the breaking of a single spring and K_{max} is the value beyond which unstable, abrupt fracturing of the sample is observed. Fatigue calculations are made by cycling the sample between $K_1 = 0$ and some K_2 . It is clear that to have a non trivial effect K_2 must satisfy $K_{min} < K_2 < K_{max}$, and then the largest possible range between K_{min} and K_{max} will be the most appropriate situation for a good modeling. The rhomboidal lattice presented the greatest range of K_{max}/K_{min} , compared to other lattices. This property is attributed to the protruding of the plastic region ahead of the crack, reducing the stress at the crack tip and hence increasing the shielding effect. This lattice is chosen to look for further effects.

In Fig. [3] the result of crack advance per cycle as a function of K_2 is plotted (with $K_1 = 0$). Each point shown corresponds to the equilibrium advance at the same K_2 . The system has 80 horizontal rows of springs and 160 vertical columns. Here $u_{bk}/u_{nl} = 3$ is used. The crack starts propagating at $K_2 = K_{min} \sim 2.2K_{nl}$ with fractional propagation (meaning less than one spring broken per cycle, on average). The propagation rate increases until $K_{max} \sim 4.5K_{nl}$, where the crack elongates up to 30 springs per cycle. As shown in the inset, there is a wide range in which a Paris relation $N \sim \alpha(K_2)^m$ may be written, with an exponent $m \simeq 4.7$.

The relation between K_2 , the size of the plastic region and the parameter relation u_{bk}/u_{nl} will be discussed now. In Fig. [4] results similar to the previous simulations are shown, but also observing the size of the plastic region as a function of K_2 and of the crack advance per cycle. We define the plastic region size as the largest distance from the crack where plastic springs still appear, measured in lattice unities. A strong dependence of the plastic region size as a function of K_2 is seen. It is also seen that the size of the plastic region is limited by the value of u_{bk}/u_{nl} . Observe that the propagating range K_{max}/K_{min} increases as u_{bk}/u_{nl} increases.

The value obtained for the relation K_{max}/K_{min} in Fig. [3] is of order ~ 2 . Fatigue experiments, in comparison, show several orders of magnitude in this relation. The reason for this small range in the present simulations is the size of the system used. In Fig. [4] it is shown that increasing the size of the system and also the relation u_{bk}/u_{nl} , the value of K_{max}/K_{min} increases. This is due to the fact that the maximum reachable size of the plastic region depends on the relation u_{bk}/u_{nl} , as it can also be seen in the figure. In turn, to be able to use larger values of u_{bk}/u_{nl} larger systems are needed because of the proximity to the borders. In the present simulations $u_{bk}/u_{nl} < \sim 5$. Experimental values of u_{bk}/u_{nl} are expected to be of order of 100, explaining the discrepancy.

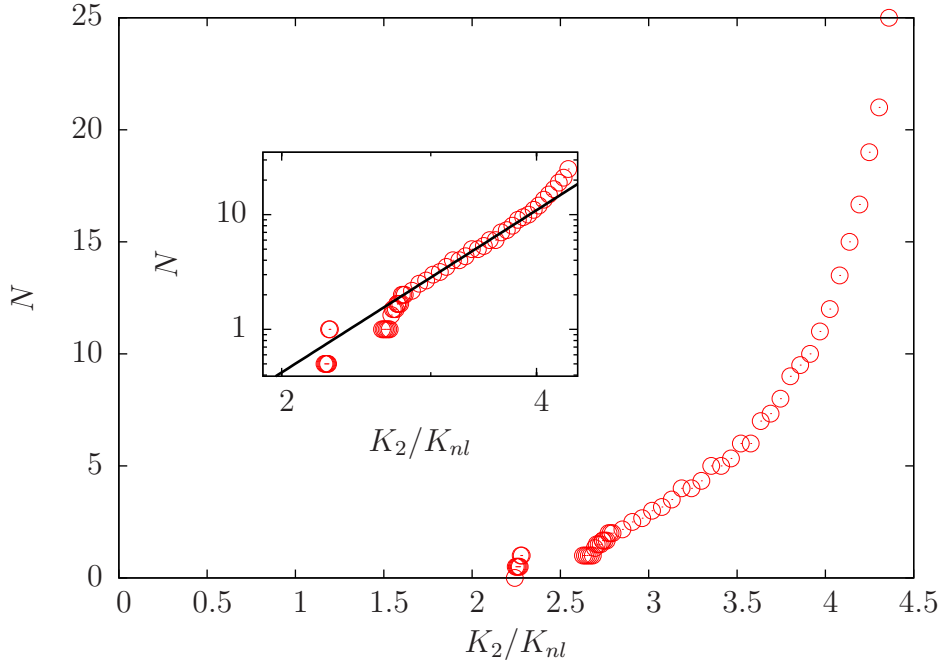


Figure 3: Paris curve for a rhomboidal lattice: number of broken springs per cycle (N) as a function of K_2 (with $K_1 = 0$). The exponent plotted in the log-log inset is 4.7. The system has 80 horizontal rows of springs, with parameters $u_{bk}/u_{nl} = 3$. K_{nl} is the stress intensity factor at which the first spring enters the plastic regime.

Overloading

One of the most interesting effects reproduced with the present modelling is the so called overloading effect. Let us a crack propagating by the fatigue mechanism, elongating n_0 lattice units per cycle, under an alternate load between 0 and K_2 . If one of the cycles is made between 0 and αK_2 with $\alpha > 1$, the advance at that cycle n'_0 is larger: $n'_0 > n_0$. However, the larger plastic region generated in this cycle shields the crack advance in the following cycles, namely $n < n_0$ after the overload. The global integrated effect is a net retardation of the propagation. The shielding may be such that the propagation is completely stopped.

In figure Fig. [5] we show the effect of four overloading cycles with $\alpha = 1.16, 1.27, 1.32$ and 1.39 . During stable cycling the crack advances $n_0 = 2.5$ springs per cycle (alternating between $n_0 = 2$ and $n_0 = 3$ springs periodically). At the overloading cycle the crack elongates a larger quantity, but smaller elongation occurs in consecutive cycles. Finally, when the stationary situation is recovered, a net retardation is seen. For $\alpha = 1.39$ the shielding is such that the crack completely stops after the overloading cycle. In the inset to Fig. [5] the nonlinear springs for $\alpha = 1.27$ are highlighted. It can be seen that the plastic region of the overload cycle is bigger, but after that the plastic region

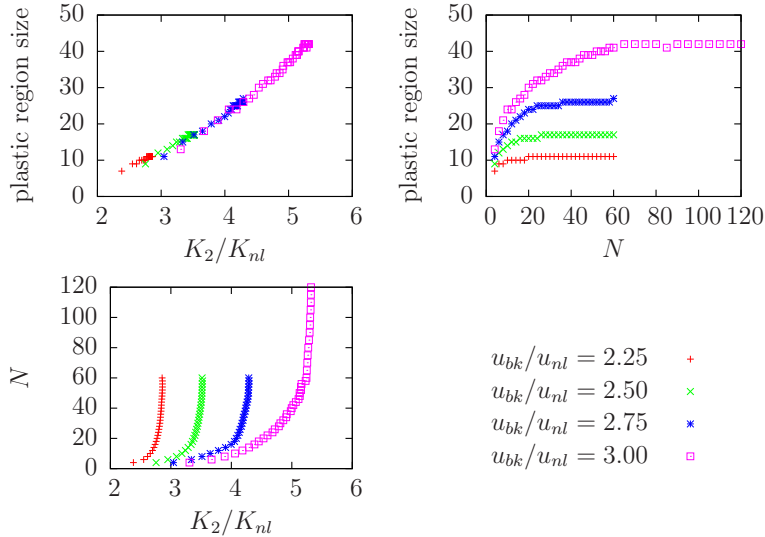


Figure 4: Results as in previous figure, showing the relation between K_2 , the size of the plastic region, the parameter relation u_{bk}/u_{nl} and the advance per cycle N . The plastic region size seems to be a function of K_2 and it is limited by the value of u_{bk}/u_{nl} . The system has 160 horizontal rows of springs.

size increases slowly to the stable cycling configuration.

Small Cracks

Another robust effect observed in experimental fatigue propagation is the interaction between the plastic regions of both tips in a short crack. This interaction diminishes the shielding effect of the plastic region and produces a proportionally larger fatigue advance for small cracks than for larger ones.

In simulations in small systems a single broken spring is usually a non negligible fraction of the total crack length. This produces that when studying the small crack effect, a uniform fatigue advance is very difficult to achieve. We thus measure an alternative quantity that provides an equivalent information, namely the length of the most stretched unbroken spring as a function of the stress intensity factor in a single stretching simulation. This is done for different values of the original crack length.

In Fig. [6] the length of the most stretched spring is plotted as a function of the stress intensity factor K . When the system does not develop plasticity ($K < K_{nl}$) the curves for different length coincide, as they should. When the springs start to explore the plastic regime, the results begin to differ. Springs at the tip in shorter cracks are elongated more than for longer cracks. This in turn makes them fail sooner than for longer cracks.

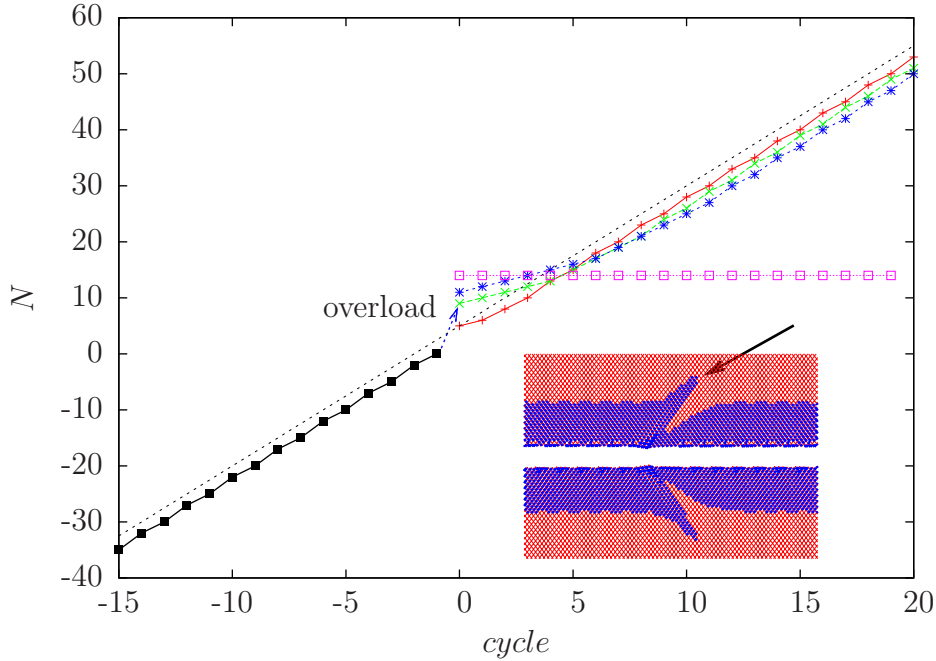


Figure 5: Number of broken springs N in fatigue propagation showing overloading effect, for $\alpha = 1.16, 1.27, 1.32$ and 1.39 . The plastic shielding created by a larger cycle diminishes the crack advance in the following cycles, such that when the system stabilizes the propagation is delayed. Contrary to intuition the effect increases upon greater overloading, and may even stop the propagation. In the inset the overload corresponding to $\alpha = 1.27$ is plotted. The arrow shows the plastic zone (highlighted springs) generated by the overload.

Borders proximity

In the previous section the enhancement at fatigue propagation when there is a limitation in the shielding of the plastic region was observed, and this was argued to represent the small crack effect. Another very similar case occurs for semi infinite crack in the middle of the stripe, for low values of the stripe width. The proximity of the borders to the plastic region diminishes its shielding property, as seen on Fig. [7]. In this figure the crack advance per cycle as a function of K_2 is plotted, like in Fig. [3], for different system sizes. When the system size is changed, the nominal stress intensity factor scales as $K \sim \delta/\sqrt{N_y}$. The values of crack advance for different system sizes agree for small values of K_2 , but differ if K_2 becomes larger, when the plastic region approaches the borders.

3 Conclusions

A method to study fatigue crack propagation that fairly reproduces well known experimental effects, such as Paris curves and overloading effect has been pre-

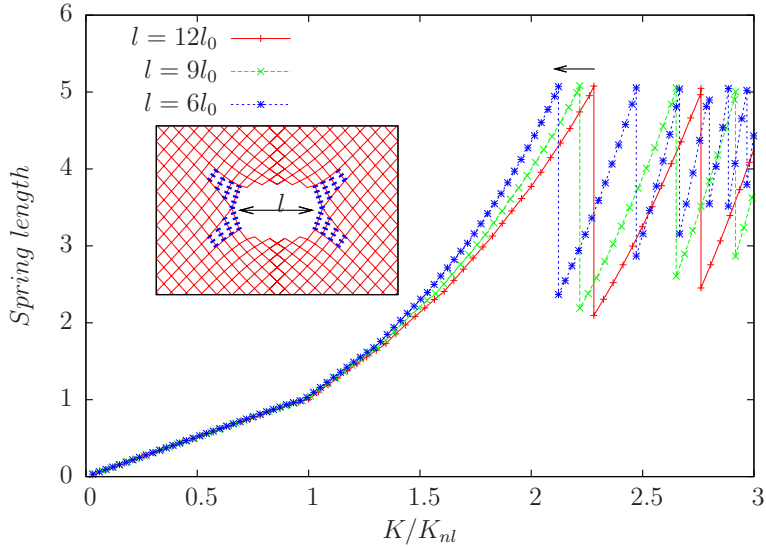


Figure 6: Length of the springs at the crack tips vs nominal K (proportional to $\delta\sqrt{l}$). Note that the smaller the crack the sooner it breaks, as shown by the arrow. Here $u_{bk}/u_{nl} = 5$, the spring length is measured in units of u_{nl} and l_0 is the lattice parameter.

sented. The model is based on a phenomenological incorporation of plasticity into a lattice spring model. We are currently working to obtain more detailed result to make quantitative comparison with experiments, and to study the fatigue phenomenon in deeper detail.

References

- [1] S. Suresh, Fatigue of Materials, Cambridge University Press, Cambridge (1998)
- [2] F. Kun, H.A. Carmona, J.S. Andrade, Jr., H.J. Herrmann, Universality behind Basquin's Law of Fatigue, Physical Review Letters 100 (2008) 094301-4

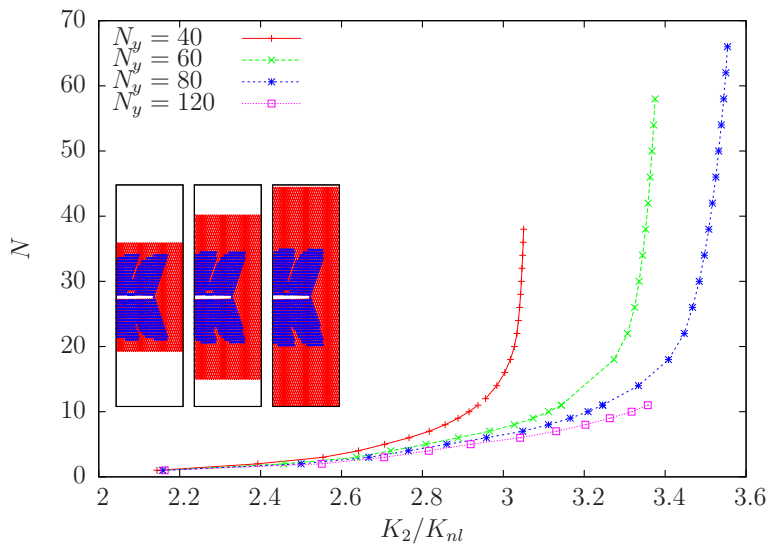


Figure 7: Crack advance as a function of K_2 in a stripe geometry for different stripe widths. For a given K_2 the advance per cycle is larger the smaller the stripe width. Inset: Snapshots of the system advancing 30 sites per cycle for system sizes $N_y = 40, 60, 80$. To keep the advancing rate as the size increases K_2 must also be increased.